

Contact Pair Dynamics During Folding of a Model Globular Protein, Hp-36

Arnab Mukherjee and Biman Bagchi

*Solid State and Structural Chemistry Unit, Indian Institute of Science, Bangalore, India 560 012.**

(Dated: November 21, 2018)

The dynamics of contact pair formation between various hydrophobic residues during folding of a model protein Hp-36 is investigated by Brownian dynamics simulation. Hydropathy scale and non-local helix propensity of amino acids are used to model the complex interaction potential. The resulting structure of the model protein mimics the native state of the real protein with a *RMSD* of 4.5 Å. A contact pair distance time correlation function (CPCF), $C_P^{ij}(t)$, is introduced which shows multistage decay, including a *slow late stage dynamics* for a few specific pairs. *These pairs determine the long time folding rate.* Dynamics can be correlated with the landscape, relative contact order and topological contact.

PACS numbers: 87.15.Aa,87.15.Cc,87.15.He,87.15.-v,83.10.Mj

The dynamics of folding of an extended protein chain at high temperature (or high urea concentration) to its unique folded state at low temperature (or low urea concentration) is a highly complex problem with many interesting aspects. Recent experimental, theoretical and computer simulations studies [1 – 7] have unearthed and explained many fascinating aspects of folding, although still many others remain to be explored. The paradigm of landscape (with the idea of folding funnel) has provided new insight into the problem [2, 5]. Experimental data on the rate of folding of a large number of small proteins have suggested a close relation between the the relative contact order and the rate of folding [7]. The relative contact order denotes the average sequence distance between the hydrophobic pair contacts and is defined as [8],

$$RCO = \frac{\sum_{i,j} (s_j - s_i)}{LN_c} \quad (1)$$

where (i, j) are the specific hydrophobic pair contacts, N_c is the number of contacts while L is total number of hydrophobic amino acids present in the protein. s_j and s_i are the sequence number along the contour of the chain. The rate of folding was found to decrease nearly exponentially with RCO . The dynamics of such non-local contact formation holds the key to the understanding of dynamics of folding. However, this aspect has remained largely unexplored.

An attractive way to explore pair dynamics of hydrophobic contact is via the technique of fluorescence resonance energy transfer (FRET). In FRET, one measures the time dependence of energy transfer from a chosen donor fluorophore to a chosen acceptor. The rate of transfer may be due to dipolar interactions and the rate of transfer is given by the well known Förster expression [9],

$$k_f = k_{rad} \left(\frac{R_F}{R} \right) \quad (2)$$

where k_{rad} is the radiative rate and R_F is the Förster radius. By suitably choosing donor-acceptor pair, R_F can be varied over a wide range. This allows the study of the dynamics of pair separation, essential to understand protein folding [10]. k_{rad} is typically less than (but of the order of) 10^9 sec^{-1} . Thus Förster transfer provides us with a sufficiently fast camera to take snapshots of the dynamics of contact pair formation.

In this study, we have studied contact formation by Brownian dynamics simulations of a model protein Hp-36 which is one of the smallest protein that folds autonomously to a stable compact ordered structure, with a large helix content [11]. Hp-36 is a subdomain of chicken villin which is implicated in the formation of microvilli in the absorptive epithelium of the gut and the proximal tube of the kidney [12]. All atom simulation study on this Hp-36 have revealed at least two pathways of folding [13]. Earlier, several studies of Hp-36 were presented using Monte Carlo technique [14] and Brownian dynamics [15].

The model studied here is constructed by taking two atoms for a particular amino acid. The smaller atom represents the backbone C_α atom of real protein while the bigger atom mimics the whole side chain residue. Construction of the model protein has been described in detail elsewhere[16]. Similar types of model (with more rigorous force field) have been introduced by Scheraga et al. recently [17]. The total potential energy function of the model protein V_{Total} is written as,

$$V_{Total} = V_B + V_\theta + V_T + V_{LJ} + V_{helix} \quad (3)$$

where V_B and V_θ are the potential contributions due to vibration of bonds and bending motions of the bond angles. Standard harmonic potential is assumed for the above two potentials with spring constants 43.0 kJ mole $^{-1}$ Å $^{-2}$ and 8.6 kJ mole $^{-1}$ Å $^{-2}$ for the bonds between backbone atoms and bonds joining side residues with the backbone atoms, respectively. In case of the bending potential, spring constant is taken to be 10.0 kJ mol $^{-1}$ rad $^{-2}$. V_T ($= \epsilon_T \sum_\phi (1/2)[1 + \cos(3\phi)]$) is taken as torsional potentials for the rotations of the bonds. $\epsilon_T = 1$ kJ mol $^{-1}$. The nonbonding potential V_{LJ} is the sum of

*Electronic address: bbagchi@sscu.iisc.ernet.in

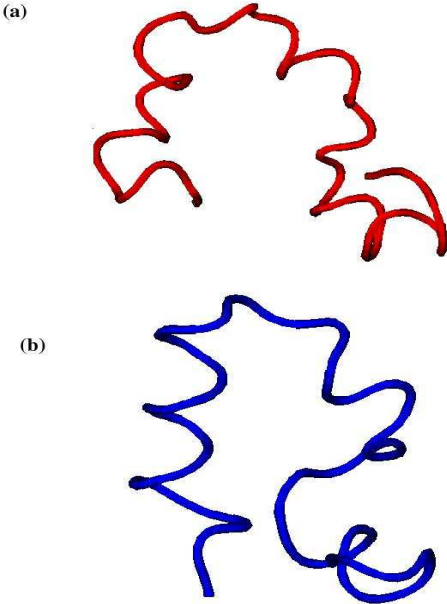


FIG. 1: (a) The backbone structure of the model protein with the lowest $RMSD$ (4.5 Å). (b) The backbone structure of the native state of real Hp-36.

the pair interactions between the atoms and is given by,

$$V_{LJ} = 4 \sum_{i,j} \epsilon_{ij} \left[\left(\frac{\sigma_{ij}}{r_{ij}} \right)^{12} - \left(\frac{\sigma_{ij}}{r_{ij}} \right)^6 \right] \quad (4)$$

where r_{ij} and ϵ_{ij} are the distance and interaction between the i -th and j -th atom. $\sigma_{ij} = \frac{1}{2}(\sigma_{ii} + \sigma_{jj})$ and $\epsilon_{ij} = \sqrt{\epsilon_{ii}\epsilon_{jj}}$. Sizes and interactions are taken to be the same (1.8 Å and 0.05 kJ mol⁻¹, respectively) for all the backbone atoms as they represent the C_α atoms in case of real proteins. Side residues, on the other hand, carry the characteristics of a particular amino acid. Different sizes of the side residues are taken from the values given by Levitt [18]. Interactions of the side residues are obtained from the hydrophobicities of the amino acids. We construct effective potential guided by the well-known statistical mechanical relation between potential of mean force and radial distribution function as $V_{ij}^{eff} = -k_B T \ln g_{ij}(r)$ [19]. Strong correlation among the hydrophobic groups (absent among the hydrophilic amino acids) implies that the hydrophobic amino acids should have stronger effective interaction than the hydrophilic groups. So the interaction parameters of the side residues can be mapped from the hydropathy scale [20] by using a linear equation as given below,

$$\epsilon_{ii} = \epsilon_{min} + (\epsilon_{max} - \epsilon_{min}) * \left(\frac{H_{ii} - H_{min}}{H_{max} - H_{min}} \right) \quad (5)$$

where, ϵ_{ii} is the interaction parameter of the i th amino acid with itself. ϵ_{min} (=0.2 kJ mol⁻¹) and ϵ_{max} (=11.0 kJ mol⁻¹) are the minimum and maximum value of the interaction strength chosen for the most

hydrophilic(arginine) and most hydrophobic(isoleucine) amino acids, respectively. H_{ii} is the hydropathy index of i th amino acid given by Kyte and Doolittle [20] and H_{min} (=−4.5) and H_{max} (=4.5) are the minimum and maximum hydropathy index among all the amino acids. Further details are available in Ref. 16. An important

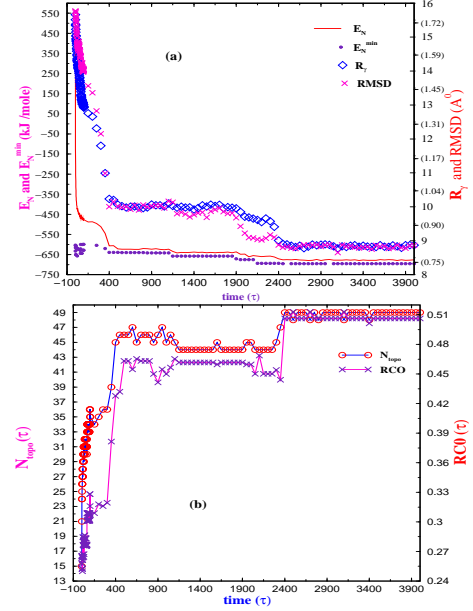


FIG. 2: (a) The multistage temporal evolution of energy E_N and minimized energy E_N^{min} (left ordinate), radius of gyration R_γ (right ordinate) and $RMSD$ (right ordinate in parenthesis) are plotted in the same time axis to show the dynamical correlation. (b) Dynamics of the topological contact N_{topo} (left ordinate) and the RCO (right ordinate) are plotted in the same time axis which show a similar dynamical growth.

part of secondary structure of the real protein is the formation of α helix. In the absence of hydrogen bonding, we introduce the following effective potential among the backbone atoms to mimic the helix formation along the chain of residues that show high helix propensity,

$$V_{helix} = \sum_{i=3}^{N-3} \left[\frac{1}{2} K_i^{1-3} (r_{i,i+2} - r_h)^2 + \frac{1}{2} K_i^{1-4} (r_{i,i+3} - r_h)^2 \right] \quad (6)$$

where $r_{i,i+2}$ and $r_{i,i+3}$ are the distances of i th atom with $i+2$ and $i+3$ th atoms, respectively. r_h is the equilibrium distance and is taken as 5.5 Å, motivated by the observation that the distance of r_i with r_{i+2} and r_{i+3} is nearly constant at 5.5 Å in an α helix. The summation excludes the first and last three amino acids as there is less helix formation observed in the ends of the protein chain [21]. The force constant for the above harmonic potential is mapped from the helix propensities Hp_i taken from Scholtz *et al.* [22], $K_i = K_{alanine} - Hp_i \times (K_{alanine} - K_{glycine})$. $K_{alanine}$ and $K_{glycine}$ are the force constants for alanine and glycine, 17.2 and 0.0 kJ mol⁻¹, respectively. Next, the influence of the neighboring amino acids for the formation

of helix has been considered by taking an average of the spring constants as $K_i^{1-3} = \frac{1}{3}[\mathcal{K}_i + \mathcal{K}_{i+1} + \mathcal{K}_{i+2}]$ and $K_i^{1-4} = \frac{1}{4}[\mathcal{K}_i + \mathcal{K}_{i+1} + \mathcal{K}_{i+2} + \mathcal{K}_{i+3}]$, with the condition that $K_i^{1-3}, K_i^{1-4} \geq 0$ as the force constant must remain positive. The above formulation of helix potential is motivated by the work of Chou and Fasman about the prediction of helix formation that *the neighbors of a particular amino acid* should be considered rather than its own helix propensity [23].

Figure 1(a) shows the best folded structure obtained in our simulations while figure 1(b) shows the real one. The *RMSD* calculated over backbone with the real native Hp-36 is 4.5 Å which is reasonable for such a simplified model. The initial configuration of the model protein was generated by configurational bias Monte Carlo technique [24]. Atoms attached to a single branch point were generated simultaneously. Then the initial configuration was subjected to Brownian dynamics simulation for the study the folding. Time evolution of the model protein was carried out according to the motion of each bead as below,

$$\mathbf{r}_i(t + \Delta t) = \mathbf{r}_i(t) + \frac{D_i}{k_B T} \mathbf{F}_i(t) \Delta t + \Delta \mathbf{r}_i^G \quad (7)$$

where each component of $\Delta \mathbf{r}_{i\alpha}^G$ is taken from a Gaussian distribution with mean zero and variance $\langle (\Delta r_{i\alpha}^G)^2 \rangle = 2D\Delta t$ [19, 25]. $\mathbf{r}_i(t)$ is the position of the i th atom at time t and the systematic force on i th atom at time t is $\mathbf{F}_i(t)$. The time step Δt is taken as 0.001. D_i is the diffusion coefficient of the i -th particle calculated from the Stokes-Einstein relation $D_i = \frac{k_B T}{6\pi\eta R_i}$. R_i is the radius of the i -th atom and η is the viscosity of the solvent. k_B and T are the Boltzmann constant and temperature, respectively. Simulations have been carried out for \mathcal{N} number of different initial configurations, where $\mathcal{N} = 584$.

The potential energy E_N , the radius of gyration R_g and the *RMSD* (calculated over backbone from the real native structure of Hp-36 obtained from protein data bank [11, 26]) all exhibit the multistage dynamics as shown in figure 2(a) in the same time axis. There is an initial sharp hydrophobic collapse followed by a slower decay is observed till 500τ (≈ 200 ns). A long plateau follows in the final stage which exists for a very long time ($2000\tau \approx 1\mu\text{s}$) before the protein reaches its final lowest energy state at around 2400τ . Energy values of the corresponding inherent structures obtained by conjugate gradient is shown by the symbols *which depicts the decreasing local minima attained by the system until it reaches the final folded state*. Total number of hydrophobic topological contact N_{topo} and relative contact order RCO are plotted in figure 2(b). N_{topo} is defined to be formed if two hydrophobic side chain residues come within a distance of 8.5 Å. RCO is calculated from Eq. 1. Both N_{topo} and RCO show a multistage increase signifying the participation of nonlocal contacts.

Folding can be probed microscopically by monitoring the dynamics of separation between different amino acid pairs. The widely different time scales of movement of

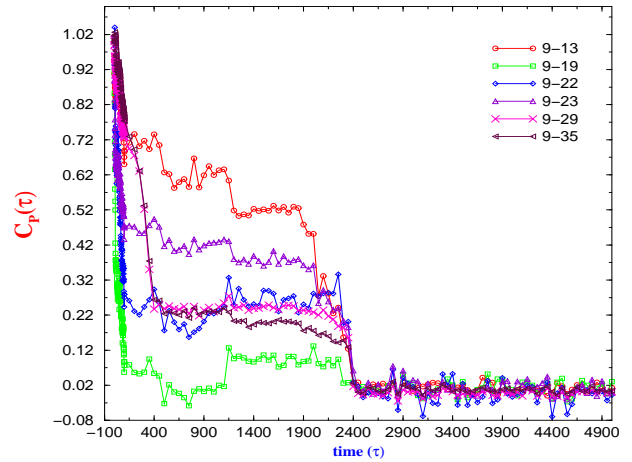


FIG. 3: Dynamics of contact formation of different side residues with the 9-th side residue is shown. The multistage relaxation process in the dynamical quantities originates from the diverse dynamics of the contact pairs.

all the different pairs together give rise to an overall picture of the dynamics of folding which is reflected in the macroscopic quantities. The effective dynamics of pair separation can be described by introducing a new pair correlation function defined below [15],

$$C_P^{ij}(t) = \frac{d^{ij}(t) - d^{ij}(\infty)}{d^{ij}(0) - d^{ij}(\infty)} \quad (8)$$

where, $d^{ij}(t) = |\mathbf{r}_i(t) - \mathbf{r}_j(t)|$. \mathbf{r}_i and \mathbf{r}_j are the positions of the i -th and j -th atom, respectively. Figure 3 shows the $C_P^{ij}(t)$ of the 9th side residue with many other hydrophobic side residues. The three stages of the folding process are reflected by mainly three different dynamical behavior seen amongst the side residues. Side residues closed to the tagged one collapse very fast. Some show an initial shoulder and only a few show the plateau in the long time decay *that correlates with the similar plateau observed in case of other dynamical quantities*. The final decrease in energy is observed when all the different contact pair correlation functions decay at around 2400τ .

We have calculated survival probability $S_P(t)$ in FRET using Förster energy transfer rate from Eq. 2 for the 9–35 pair along the Brownian dynamics trajectory leading to the most stable structure. The Förster radius R_F is taken as 10 Å. Figure 4 shows initial very slow decrease of $S_P(t)$ to be followed by a sudden drop at around 2400τ as seen in case of the different dynamical properties discussed above. $S_P(t)$ is found to be relatively insensitive to k_{rad} . The resemblance with the real native state of the protein and the dynamics of *RMSD* show the validity of the model used for this protein. Contact pair dynamics and the time evolution of energy, radius of gyration, relative contact order formation etc. brings out the rich and diverse dynamics of protein folding. The initial ultrafast hydrophobic collapse signify that the upper part of the funnel is steep – followed by a change in slope. *Rate determining step, however, arises from the final stage of*

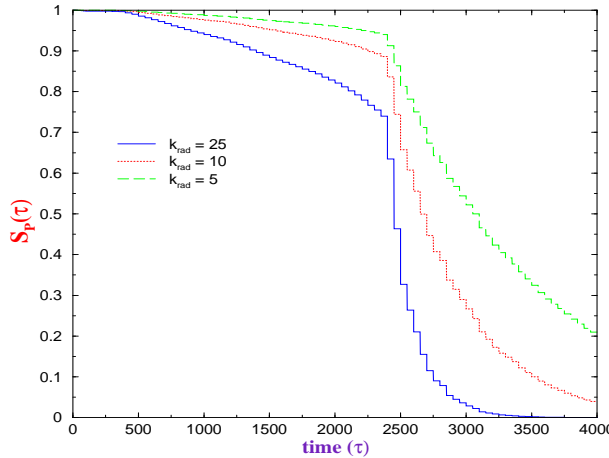


FIG. 4: FRET survival probability for $R_F = 10.0 \text{ \AA}$ is plotted for different radiative rates to capture the wide variety of time scales involved in FRET.

folding on a very flat and rugged underlying landscape marked by the large conformational entropy barrier with little energy change [6]. This entropic bottleneck arises from the necessity to form long range hydrophobic contacts, as envisaged by Dill and Wolynes. The atoms mimicking the whole side chain of the real protein play a very important role for structural and dynamical aspects in this study. Moreover, the new contact pair correlation function and FRET probes the folding events in minute detail.

A. Mukherjee thanks Ashwin, Kausik and Prasanth for technical discussions. Authors thank CSIR, New Delhi, India and DST, India for financial support.

[1] C. B. Anfinsen, *Science* **181**, 223 (1973).
[2] H. Frauenfelder, S. G. Sligar and P. G. Wolynes, *Science*, **254**, 1598 (1991).
[3] K. A. Dill, D.O.V. Alonso, and K. Hutchinson, *Biochemistry* **28**, 5439 (1989) ; K. A. Dill and H. S. Chan, *Nat. Str. Biol.* **4**, 10 (1997).
[4] P. E. Leopold, M. Montal and J. N. Onuchic, *Proc. Natl. Acad. Sci. U.S.A.* **89**, 8721 (1992).
[5] J. D. Bryngelson, M. Montal and J. N. Soccia and P. G. Wolynes, *PROTEINS : Structure, Function and Genetics*, **21**, 167 (1995) ; J. D. Bryngelson and P. G. Wolynes, *J. Phys. Chem.* **93**, 6902 (1989).
[6] R. Zwanzig, *Proc. Natl. Acad. Sci. U.S.A.* **92**, 9801 (1995).
[7] V. Grantcharova, E. J. Alm, D. Baker and A. L. Horwich, *Curr. Open. Struct. Biol.* **11**, 70 (2001).
[8] K. W. Plaxco, K. T. Simons and D. Baker, *J. Mol. Biol.* **277**, 985 (1998).
[9] Th. Förster, *Ann. Phys. (Leipzig)* **2**, 55 (1948).
[10] J. R. Telford, P. Wittung-Stafshede, H. B. Gray and J. R. Winkler, *Acc. Chem. Res.* **31**, 755 (1998) ; T. Pascher, J. P. Chesick, J. R. Winkler, and H. B. Gray, *Science* **271**, 1558 (1996).
[11] C. J. McKnight, D. S. Doering, P. T. Matsudaria and P. S. Kim, *J. Mol. Biol.* **260**, 126 (1996).
[12] A. Bretscher and K. Weber, *Proc. Natl. Acad. Sci. U.S.A.*, **76**, 2321 (1979).
[13] Y. Duan and P. A. Kollman, *Science* **282**, 740 (1998).
[14] U. H. E. Hansmann, L. T. Wille, *Phys. Rev. Lett.* **88**, 68105 (2002).
[15] G. Srinivas and B. Bagchi, *J. Chem. Phys.* **116**, 8579 (2002) ; *ibid* *Theo. Chem. Accts. (in press)*.
[16] A. Mukherjee and B. Bagchi, *J. Chem. Phys. (submitted)*.
[17] A. Liwo, S. Oldziej, M. R. Pincus, R. J. Wawak, S. Rackovský, H. A. Scheraga, *J. Comput. Chem.* **18**, 850 (1997).
[18] M. Levitt and A. Warshel, *Nature* **253**, 694 (1975) ; M. Levitt, *J. Mol. Biol.* **104**, 59 (1976).
[19] J. P. Hansen and I. R. McDonald. *Theory of Simple Liquids*, (Academic Press, 1986).
[20] J. Kyte and R. F. Doolittle, *J. Mol. Biol.* **157**, 105 (1982).
[21] B. H. Zimm and J. K. Bragg, *J. Chem. Phys.* **31**, 526 (1959).
[22] C. N. Pace and J. M. Scholtz, *Biophys. J.* **75**, 422 (1998).
[23] P. Y. Chou and G. Fasman, *Biochemistry* **13**, 211 (1974).
[24] G. C. A. M. Mooij, D. Frenkel and B. Smit, *J. Phys. Cond. Matt.* **4**, L255 (1992) ; D. Frenkel and B. Smit, *Mol. Phys.* **75**, 983 (1992).
[25] D. L. Ermak and J. A. McCammon, *J. Chem. Phys.* **69**, 1352 (1978).
[26] F. C. Bernstein, T. F. Koetzle, G. J. B. Williams, E. F. Meyer, M. D. Brice, J. R. Rodgers, O. Kennard, T. Shimanouchi and M. Tasumi, *J. Mol. Biol.* **112**, 535 (1977)